Available online at www.sciencedirect.com
SCIENCE DIRECT
Optics Communications 264 (2006) 435–440
OPTICS COMMUNICATIONS
www.elsevier.com/locate/optcom

Adiabatic passage with superconducting nanocircuits

Jens Siewert [a,b,*], Tobias Brandes [c], Giuseppe Falci [a]

[a] MATIS-INFM, Consiglio Nazionale delle Ricerche, and Dipartimento di Metodologie Fisiche e Chimiche per l'Ingegneria, Universita di Catania, I-95125 Catania, Italy
[b] Institut für Theoretische Physik, Universität Regensburg, D-93040 Regensburg, Germany
[c] Department of Physics, The University of Manchester, Manchester, United Kingdom

Received 3 November 2005; accepted 14 December 2005

Abstract

Superconducting nanocircuits are macroscopic solid-state systems that exhibit quantum-coherent dynamics. In particular it is possible to design such circuits that display the behavior of few-level systems. It is an interesting question whether the scheme of stimulated Raman adiabatic passage (STIRAP) can be transferred to these systems. Here we discuss various possibilities to achieve quantum control with this powerful method for devices in the charge regime and assess the effect of decoherence on their functionality.

Keywords: STIRAP; Superconducting nanocircuits; Macroscopic quantum coherence

1. Introduction

It has been envisioned several decades ago that superconducting circuits containing Josephson junctions may exhibit the dynamics of quantum systems [1–4]. The experimental verification of this fact was achieved by Nakamura et al. for charge qubits [5] and subsequently by a number of experimental groups for other superconducting nanocircuits in various designs and regimes [6–9].

It has become clear from the outset that this area of solid-state research could benefit significantly from the rich experience of controlling single quantum objects in fields like nuclear magnetic resonance and quantum optics. In fact, in the first experiments well-known techniques such as Rabi oscillations, spin-echo experiments, observation of Ramsey fringes, etc. were used in order to prove the quantum dynamics of such objects as well as to determine system parameters such as decoherence and dephasing times.

Naturally one may expect that also more complex methods and topics from quantum optics find their "analogue" for superconducting nanocircuits. An important step in this direction has been taken by Wallraff et al. [9] and Blais et al. [10] who showed that *cavity*-QED may be "translated" to *circuit*-QED in a straightforward manner (see also the experiments by Chiorescu et al. [11] and Johansson et al. [12]). In these realizations of circuit-QED an important advantage of superconducting nanocircuits is exploited: there is a variety of methods to "tailor" the appropriate few-level system and the available coupling parameters such as the coupling between the superconducting qubit (the artificial two-level atom) and the superconducting resonator (the cavity). For example, in the experiment of Ref. [9] the ratio of vacuum Rabi frequency and transition frequency was chosen to be about three orders of magnitude larger than for typical microwave or optical cavities.

Stimulated Raman adiabatic passage (STIRAP) is another well-established technique that has numerous applications in quantum optics and beyond this field [13,14]. Until now, methods based on STIRAP are quite rare in solid-state physics. There have been proposals for quantum-dot devices, e.g., Refs. [15–17], superconducting

* Corresponding author. Address: MATIS-INFM, Consiglio Nazionale delle Ricerche, and Dipartimento di Metodologie Fisiche e Chimiche per l'Ingegneria, Universita di Catania, I-95125 Catania, Italy.
E-mail address: jsiewert@dmfci.ing.unict.it (J. Siewert).

0030-4018/$ - see front matter © 2006 Elsevier B.V. All rights reserved.
doi:10.1016/j.optcom.2005.12.083

circuits in the charge regime [18–20] and in the phase and flux regimes [21,22]. A particularly interesting idea is to use adiabatic passage to obtain population transfer between different states of a many-body quantum system [23].

In this contribution, we discuss two basic realizations of STIRAP in superconducting circuits in the charge regime. We highlight the analogies and also the differences with STIRAP in three-level atoms. We consider also the effect of decoherence and find a remarkable robustness of the method. Further, it is an objective of this work to investigate whether typical parameter ranges for charge devices are suitable for the experimental verification of STIRAP.

2. Brief reminder of STIRAP with three-level atoms

To fix ideas and to introduce some notation we briefly review the conventional STIRAP technique. It uses atoms with three energy levels ε_e, ε_1, ε_0 in a Λ configuration (the corresponding states are $|e\rangle$, $|1\rangle$ and $|0\rangle$). By applying laser fields $(A_0/2)\cos\omega_0 t$, $(A_1/2)\cos\omega_1 t$ with frequencies close to those of the atomic transitions $|0\rangle \to |e\rangle$ and $|1\rangle \to |e\rangle$ the energy levels are coupled (here $A_0/2$, $A_1/2$ represent the coupling strengths due to the atomic dipole moments). The corresponding Hamiltonian written in the basis $\{|e\rangle,|1\rangle,|0\rangle\}$ can be transformed to the rotating frame (by applying the rotating-wave approximation)

$$H = \frac{1}{2}\begin{bmatrix} 2\varepsilon_e & A_1\cos\omega_1 t & A_0\cos\omega_0 t \\ A_1^*\cos\omega_1 t & 2\varepsilon_1 & 0 \\ A_0^*\cos\omega_0 t & 0 & 2\varepsilon_0 \end{bmatrix} \to H_{\text{r.f.}} = \frac{1}{2}\begin{bmatrix} 2\Delta & A_1 & A_0 \\ A_1^* & 0 & 0 \\ A_0^* & 0 & 0 \end{bmatrix}, \tag{1}$$

where we have introduced the detuning $\Delta = (\varepsilon_e - \varepsilon_0) - \omega_0 = (\varepsilon_e - \varepsilon_1) - \omega_1$. The dark state $|D\rangle = A_0|1\rangle - A_1|0\rangle$ (not normalized) can be used for population transfer from state $|0\rangle$ to state $|1\rangle$ with the so-called counterintuitive scheme. By preparing the system in the state $|0\rangle$ with $A_0 = 0$, $A_1 \neq 0$ the dark state can be rotated by slowly switching on the coupling A_0, and simultaneously switching off the coupling A_1. Adiabaticity is achieved for $|\dot{A}_j/A_j| < |A_j|$.

3. STIRAP with superconducting nanocircuits

Before we discuss possibilities for the implementation of STIRAP with superconducting nanocircuits we explain in a nutshell how quantum-coherent dynamics arises in such circuits.

3.1. Quantum dynamics of charges in a Cooper-pair box

The simplest superconducting nanocircuit is the so-called Cooper-pair box (CPB), see Fig. 1a. The system is investigated experimentally at ultra-low temperatures (<100 mK) such that all parts of the circuit (typically made of aluminum) are superconducting and there are no quasiparticles in the system. The dynamical variable is the (discrete) charge number n (i.e., the number of excess Cooper-pair charges $2e$) on the superconducting island (or, respectively, the phase difference φ across the Josephson junction). Charge and phase can be regarded as conjugate variables [1,4].

The Hamiltonian of the CPB is

$$H = E_C(n - n_g)^2 - E_J\cos\varphi, \tag{2}$$

where the first term on the r.h.s. represents the electrostatic energy and the second term describes the Josephson junction. The representation of charge states is related to that of the phase states via the relation $|\varphi\rangle = \sum_n e^{in\varphi}|n\rangle$ [24] and the Hamiltonian can be rewritten in terms of charge states

$$H = \sum_n E_C(n - n_g)^2|n\rangle\langle n| - \frac{E_J}{2}(|n\rangle\langle n+1| + \text{h.c.}). \tag{3}$$

This is convenient in particular if $E_C \gg E_J$, i.e., for the so-called charge regime. The opposite limit is termed flux (or phase) regime. From Eq. (3) we see that the circuit in the charge regime can be considered as a discrete quantum system, in analogy, e.g., with an atom.[1] We mention that also more complicated circuits (and different regimes) can be analyzed in a similar way, i.e., their Hamiltonian displays one or more pairs of conjugate charge and phase variables in analogy with Eq. (2) such that by choosing a proper representation these systems can be viewed as discrete few-level systems.

3.2. STIRAP with a single Cooper-pair box

Once we have shown that the CPB represents a discrete quantum system, we can turn to constructing a STIRAP procedure. Consider Fig. 1c where we have plotted the lowest energy levels of the CPB circuit as a function of the gate charge n_g (which is constant in time). In principle we can choose any value of n_g as the working point and perform STIRAP, e.g., from the ground state to the first excited state via the second excited level. We need to mention, however, that one needs to exclude the vicinity of symmetry points $n_g = k + 1/2$ (with k an integer). At these points, the level separation may become rather small and, moreover, the parity of the wavefunctions induces selection rules (see also Ref. [25]).

In order to realize adiabatic passage with this setup we need to couple two driving fields that induce the Raman transition. This can be done by adding a small ac part to the gate charge (i.e., to the gate voltage):

[1] Therefore, one may find the term "artificial atom" for such circuits.

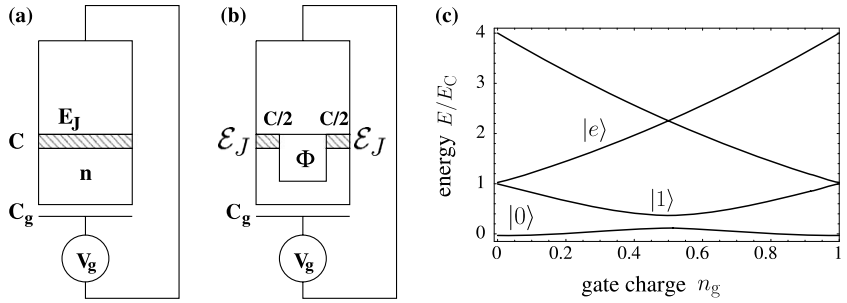

Fig. 1. (a) Circuit of the Cooper-pair box. A superconducting island with a charge of n excess Cooper pairs is connected via a Josephson junction (capacitance C, Josephson energy E_J) to a superconducting lead. The potential of the island can be controlled with the voltage V_g via the gate capacitance C_g. With the (continuous) offset charge $n_g \equiv C_g V_g/(2e)$ the electrostatic energy of the circuit can be written as $\mathscr{E}(n) = E_C(n - n_g)^2$ with the so-called charging energy $E_C \equiv \frac{(2e)^2}{2(C+C_g)}$. Typical values for the total island capacitance are on the order of $\sim 10^{-15}$ F which lead to a charging energy of ~ 400 μV. (b) CPB with a tunable Josephson junction. Due to the SQUID layout of the junction the Josephson energy depends on the external magnetic flux Φ: $E_J(\Phi) = 2\mathscr{E}_J \cos\frac{e\Phi}{\hbar}$. (c) The four lowest energy levels of a CPB as a function of gate charge for a ratio $E_J/E_C = 0.25$. STIRAP can be performed between the states $|0\rangle$, $|1\rangle$, $|e\rangle$.

$$n_g(t) = n_{g0} + n_g^{ac}(t),$$
$$n_g^{ac}(t) = A_0 \cos\omega_0 t + A_1 \cos\omega_1 t$$

with $A_j \ll 1$. Note the important fact that the driving fields appear on the diagonal of the Hamiltonian equation (3) (in contrast to the three-level atom equation (1)). That is, without mixing of the charge states due to the Josephson coupling the driving fields could not induce any transition.

As the initial state we can choose the ground state $|0\rangle$. It is prepared by letting the system relax to thermal equilibrium. By applying Gaussian-shaped pulses of the microwave fields $A_j(t)$ in the counterintuitive sequence we can transfer the population from the initial state to the final state $|1\rangle$ as shown in Fig. 2. In order to obtain these graphs we have solved the von Neumann equation for the density matrix $\dot{\rho} = (i/\hbar)[\rho, H] + \Gamma\rho$ numerically. The solid lines represent the ideal case (no dissipation, $\Gamma\rho \equiv 0$) while the dashed lines take into account relaxation and dephasing

$$(\Gamma\rho)_{ij} = \frac{\gamma_i + \gamma_j}{2}\rho_{ij} - (1 - \delta_{ij})\tilde{\gamma}\rho_{ij} - \delta_{ij}\sum_k \rho_{kk}\gamma_{k\to i} \qquad (4)$$

with $\gamma_i = \sum_{k\neq i}\gamma_{i\to k}$. The dissipator is taken time-independent in the rotating frame (thus overestimating decoherence) and includes all transitions as well as a dephasing rate $\tilde{\gamma}$ accounting phenomenologically for low-frequency noise. For the decay rate of the second excited state we assume $\gamma_e = \gamma_{e\to 1} + \gamma_{e\to 0} = 2\gamma_1$.

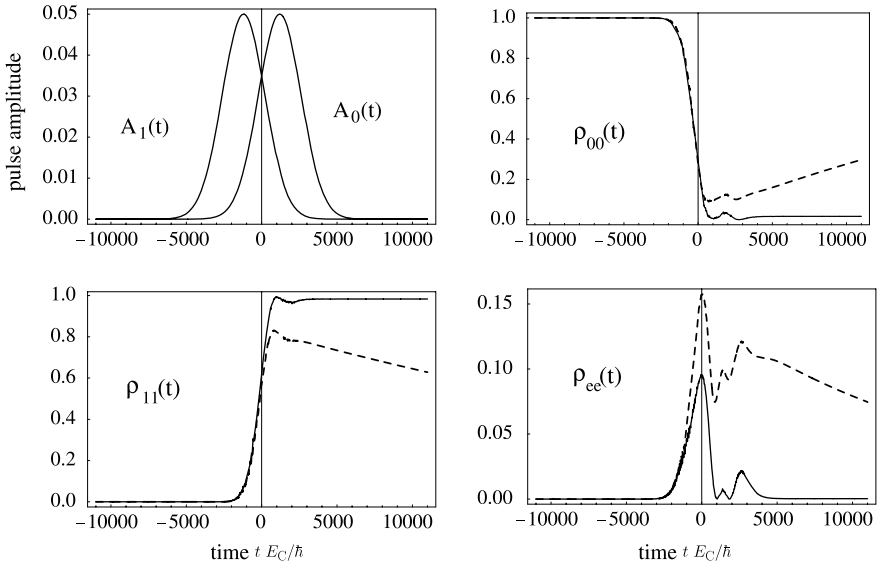

Fig. 2. Population transfer in a single CPB with $E_J/E_C = 0.25$ and zero detuning $\Delta = 0$. The working point is $n_g = 0.4$. In a typical CPB experiment one has $E_C \sim 50$ μeV, e.g., a time unit corresponds to about 1.3×10^{-11} s. Solid lines represent the diagonal elements of the density matrix for the system without dissipation, dashed lines are for a system with dissipation (see text). We have used $\gamma_1 = 3.0 \times 10^{-5}$, $\tilde{\gamma} = 2.0 \times 10^{-4}$ which correspond to typical values in an experiment. The main effect of decoherence is that the transfer is not completed as the population that arrives in state $|1\rangle$ decays to the ground state $|0\rangle$. Notice that also the population of $|e\rangle$ is increased.

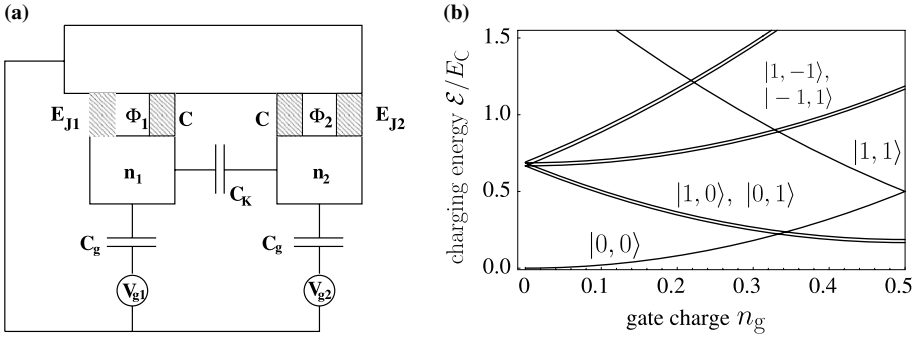

Fig. 3. (a) Two-island setup for the implementation of STIRAP. It is important that both Josephson couplings can be controlled. The same device can be used to implement two capacitively coupled charge qubits (cf., e.g., Ref. [26]). (b) Charging energy of various charge states as a function of gate charge with $C_K/C = 1.0$. We have put a small offset to the lines corresponding to degenerate charge states.

We see that population transfer with a high efficiency can be achieved even in the presence of considerable decoherence sources. Note that in this implementation population transfer does not occur between pure charge states as the Josephson coupling is always switched on. Thus, away from the symmetry points, the eigenstates are almost pure charge states with small admixtures of the neighboring charge states.

The detection of the final state is done by measuring the state of the island. Appropriate read-out devices are, e.g., a big Josephson junction [6] or a tank circuit [9].

3.3. STIRAP with two Cooper-pair boxes – without ac fields

While the implementation in the preceding section is very much analogous to STIRAP with a three-level atom, one can also realize the Hamiltonian directly in the rotating frame (see Eq. (1)). That is, no ac driving fields are required in this case. The corresponding circuit consists of two capacitively coupled CPBs and is shown in Fig. 3. The coupling capacitance C_K is, apart from its presence in real circuits, necessary in order to break symmetries of the spectrum that could hamper the STIRAP procedure.

The dynamical variables are the charge numbers n_1 and n_2 of the two islands. We assume equal junction capacitances C. In real devices, the gate capacitance is often much smaller than the junction capacitances $C_g \ll C$. With these simplifications, the electrostatic energy of the circuit is

$$\mathscr{E}(n_1,n_2) \simeq E_C\left\{\frac{C+C_K}{C+2C_K}\left[(n_1-n_{g1})^2+(n_2-n_{g2})^2\right] + \frac{2C_K}{C+2C_K}(n_1-n_{g1})(n_2-n_{g2})\right\}. \quad (5)$$

Here, $E_C = (2e)^2/(2C)$. The system can be characterized with the basis of charge states $\{|n_1,n_2\rangle\}$ where $|n_1,n_2\rangle \equiv |n_1\rangle \otimes |n_2\rangle$. Consider gate charges $n_{g1} = n_{g2} = n_g \lesssim 1/2$. Then, states $|n_1,n_2\rangle$ with $n_1,n_2 \in \{0,1\}$ have the lowest charging energy (see also Fig. 3b). Including these four states and their Josephson couplings, the Hamiltonian in the basis $\{|0,0\rangle, |0,1\rangle, |1,0\rangle, |1,1\rangle\}$ reads

$$H = E_C\begin{bmatrix} -(1-2n_g)+\frac{C_K}{C+2C_K} & -\frac{E_{J2}}{2E_C} & -\frac{E_{J1}}{2E_C} & 0 \\ -\frac{E_{J2}}{2E_C} & 0 & 0 & -\frac{E_{J1}}{2E_C} \\ -\frac{E_{J1}}{2E_C} & 0 & 0 & -\frac{E_{J2}}{2E_C} \\ 0 & -\frac{E_{J1}}{2E_C} & -\frac{E_{J2}}{2E_C} & (1-2n_g)+\frac{C_K}{C+2C_K} \end{bmatrix}. \quad (6)$$

We see that $\mathscr{E}(0,1) = \mathscr{E}(1,0)$. Further, the energy of the fourth state $|1,1\rangle$ is by an amount of the order $\sim E_C > E_{Jj}$ further away from $\mathscr{E}(0,1)$ than that of the state $|0,0\rangle$. Therefore, we can implement an adiabatic population transfer $|1,0\rangle \to |0,1\rangle$ as follows.

We prepare (by appropriate switching of gate voltages) the state $|1,0\rangle$ (i.e. one excess Cooper pair on the left island) and switch off the left Josephson coupling $E_{J1}(t=0) = 0$ while the right coupling is non-zero $E_{J2}(t=0) \neq 0$. Then we slowly turn off the right coupling E_{J2} and, simultaneously, switch on E_{J1}. The procedure terminates when the right coupling is completely switched off. During the procedure the excess Cooper pair is transferred from the left to the right island. Again, we can use also Gaussian-shaped functions for $E_{Jj}(t) = E_J \exp\left[-\left(\frac{t-t_{delj}}{T}\right)^2\right]$ as long as the pulses are applied in the counterintuitive. sequence. Here, T characterizes the pulse width and t_{delj} is the delay time of the jth pulse.

If the couplings are set to zero at the beginning and the end of the transfer, ideally *exactly* one (Cooper-pair) charge is transferred between the islands. It is remarkable that this does not depend on the state of the lead.[2] However, we need to mention here that the experimental realization of this procedure is difficult. A two-island setup is even more sensitive to background-charge fluctuations than an experiment with a single CPB [27]. Further, with current technological solutions it is hard to really switch off a Josephson junction; typically E_J can only be reduced to a few percent of its maximum value. Nevertheless, the

[2] It is straightforward to check explicitly that the result does not change for any superposition of lead charge states. Note that, after all, also the single CPB as a two-level system does not display any dependence on the state of the lead.

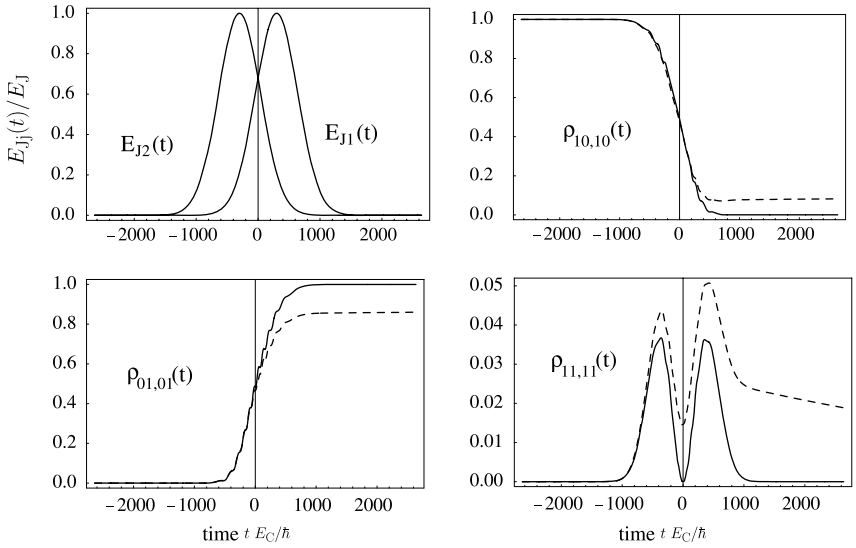

Fig. 4. Population transfer with the setup in Fig. 3 with $E_J/E_C = 0.25$ using Gaussian pulse shape for $E_{Jj}(t)$. The working point is $n_g = 0.4$ and the capacitance ratio $C_K/C = 1.0$. Solid lines are results without decoherence; dashed lines describe the system with decoherence. We have used identical relaxation rates for all transitions between charge states $\gamma_{i\to k} \equiv \gamma = 6.0 \times 10^{-5}$ (constant in time) which for $E_C \sim 50$ μV corresponds to a relaxation time of the first excited state $|0,0\rangle$ of ~200 ns. For dephasing we have used $\tilde{\gamma} = 4.0 \times 10^{-4}$. We observe that during the STIRAP procedure the population is distributed among many higher charge states (as an example we have plotted the population of the state $|1,1\rangle$).

STIRAP experiment can be carried out. The only difference is that, instead of pure charge states, one has almost pure charge states with small admixtures (with amplitudes $\sim E_J/E_C$ of adjacent charge states) in the initial and final state.

In Fig. 4 we show the time evolution of the relevant diagonal elements of the density matrix for the two-island implementation of STIRAP. Also in this case we note the remarkable robustness of the procedure with respect to decoherence.

4. Conclusion

In summary, we have discussed the possibility to implement stimulated Raman adiabatic passage with superconducting nanocircuits in the charge regime. Essentially we have presented two versions of STIRAP, on the one hand an implementation that is driven by microwaves and that is very much analogous to STIRAP in a three-level atom. On the other hand, STIRAP can also be implemented by tailoring the rotating-frame Hamiltonian of the three-level atom. The latter implementation does not require microwave sources. With both schemes it is possible to achieve highly efficient population transfer that is robust against the action of decoherence.[3]

One goal of this discussion is to provide a simple basis and parameter estimates for the experimental realization of STIRAP in superconducting nanocircuits. As we have shown, the implementations use standard circuit designs with rather common parameters and corresponding time scales. Consequently, it should be feasible to experimentally verify stimulated Raman adiabatic passage in nanocircuits with state-of-the-art technology.

Of course, there are interesting potential applications of this scheme. One possibility to apply the microwave-driven implementation is in quantum-state engineering similar to quantum optics, e.g., for the preparation of Fock states of resonators coupled to the nanocircuit [20]. Another idea for an application is imposed by the implementation in Section 3.3. If both couplings are switched off before and after the population transfer, one can be sure that an integer number of charges has passed from one island to the other. That is, precise charge pumping is another possible solid-state application of STIRAP.

[3] We mention that the simultaneous presence of high-frequency and low-frequency noise components in superconducting circuits render the action of decoherence in these systems qualitatively different from that in quantum optics. Its investigation is an interesting topic in its own right.

Acknowledgments

This work has been supported financially by SFB 631 of the DFG. J.S. received financial support from the Heisenberg program of the DFG. The authors would like to thank K. Bergmann, A. Kuhn and M. Storcz for illuminating discussions and T. Duty and D. Esteve for stimulating comments.

References

[1] V. Ambegaokar, U. Eckern, G. Schön, Phys. Rev. Lett. 48 (1982) 1745.
[2] A.O. Caldeira, A.J. Leggett, Ann. Phys. (N.Y.) 149 (1983) 374.
[3] M.H. Devoret, J.M. Martinis, J. Clarke, Phys. Rev. Lett. 55 (1985) 1908.
[4] Y. Makhlin, G. Schön, A. Shnirman, Rev. Mod. Phys. 73 (2001) 357.

[5] Y. Nakamura, Yu. Pashkin, J.S. Tsai, Nature 398 (1999) 786.
[6] D. Vion, A. Aassime, A. Cottet, P. Joyez, H. Pothier, C. Urbina, D. Esteve, M.H. Devoret, et al., Science 296 (2002) 886.
[7] J.M. Martinis, S. Nam, J. Aumentado, C. Urbina, Phys. Rev. Lett. 89 (2002) 117901.
[8] I. Chiorescu, Y. Nakamura, C.J.P.M. Harmans, J.E. Mooij, Science 299 (2003) 1869.
[9] A. Wallraff, D.I. Schuster, A. Blais, L. Frunzio, R.S. Huang, J. Majer, S. Kumar, S.M. Girvin, R.J. Schoelkopf, Nature 431 (2004) 162.
[10] A. Blais, R.-S. Huang, A. Wallraff, S.M. Girvin, R.J. Schoelkopf, Phys. Rev. A 69 (2004) 062320.
[11] I. Chiorescu, P. Bertet, K. Semba, Y. Nakamura, C.J.P.M. Harmans, J.E. Mooij, Nature 431 (2004) 159.
[12] J. Johansson, S. Saito, T. Meno, H. Nakano, M. Ueda, K. Semba, H. Takayanagi, Phys. Rev. Lett. 96 (2006) 127006.
[13] K. Bergmann, H. Theuer, B.W. Shore, Rev. Mod. Phys. 70 (1998) 1003.
[14] N.V. Vitanov, M. Fleischhauer, B.W. Shore, K. Bergmann, Adv. Atom. Mol. Opt. Phys. 46 (2001) 55.
[15] T. Brandes, F. Renzoni, Phys. Rev. Lett. 85 (2000) 4148;
T. Brandes, F. Renzoni, R.H. Blick, Phys. Rev. B 64 (2001) 035319.
[16] F. Renzoni, T. Brandes, Phys. Rev. B 64 (2001) 245301.
[17] A.D. Greentree, J.H. Cole, A.R. Hamilton, L.C.L. Hollenberg, Phys. Rev. B 70 (2004) 235317.
[18] L. Faoro, J. Siewert, R. Fazio, Phys. Rev. Lett. 90 (2003) 28301.
[19] J. Siewert, T. Brandes, Adv. Solid State Phys. 44 (2004) 181.
[20] J. Siewert, T. Brandes, G. Falci, e-print cond-mat/0509735, 2005.
[21] M.H.S. Amin, A.Y. Smirnov, A. Maassen van den Brink, Phys. Rev. B 67 (2003) 100508(R).
[22] E. Paspalakis, N.J. Kylstra, J. Mod. Opt. 51 (2004) 1679;
Z. Kis, E. Paspalakis, Phys. Rev. B 69 (2004) 024510.
[23] J. Fabian, U. Hohenester, e-print cond-mat/0412229, 2004.
[24] P.G. de Gennes, Superconductivity of Metals and Alloys, W.A. Benjamin, New York, 1966.
[25] Y.-X. Liu, J.Q. You, L.F. Wei, C.P. Sun, F. Nori, Phys. Rev. Lett. 95 (2005) 087001.
[26] T. Yamamoto, Yu.A. Pashkin, O. Astafiev, Y. Nakamura, J.S. Tsai, et al., Nature 425 (2003) 941.
[27] E. Paladino, L. Faoro, G. Falci, R. Fazio, Phys. Rev. Lett. 88 (2002) 228304;
G. Falci, A. D'Arrigo, A. Mastellone, E. Paladino, Phys. Rev. Lett. 94 (2005) 167002.